



Impact of silt chemical composition on deflocculation and coagulation of clay-rich paste

Journal Article

Author(s):

Ardant, Daria; [Brumaud, Coralie](#) ; Zosso, Nino; Bernard, Ellina; [Habert, Guillaume](#) 

Publication date:

2024-08-05

Permanent link:

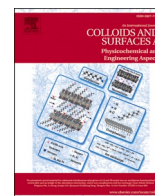
<https://doi.org/10.3929/ethz-b-000672228>

Rights / license:

[Creative Commons Attribution-NonCommercial-NoDerivatives 4.0 International](#)

Originally published in:

Colloids and Surfaces A: Physicochemical and Engineering Aspects 694, <https://doi.org/10.1016/j.colsurfa.2024.134147>



Impact of silt chemical composition on deflocculation and coagulation of clay-rich paste

Daria Ardant^{a,*}, Coralie Brumaud^a, Nino Zosso^b, Ellina Bernard^c, Guillaume Habert^a

^a Institute of Construction and Infrastructure Management, Chair of Sustainable Construction, Swiss Federal Institute of Technology (ETH Zurich), Zürich, Switzerland

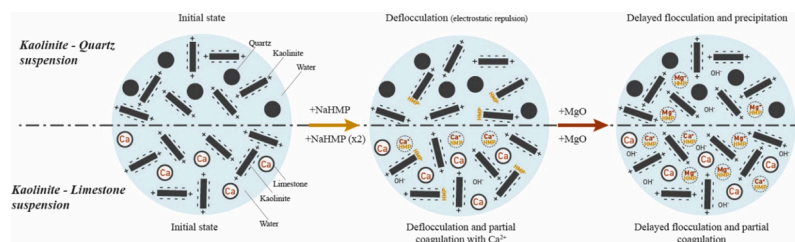
^b Department of Materials, Swiss Federal Institute of Technology (ETH Zurich), Zürich, Switzerland

^c EMPA, Swiss Federal Laboratories for Materials Science and Technology, Dübendorf, Switzerland

HIGHLIGHTS

- The deflocculation/coagulation process is affected by the chemical composition of the suspension.
- The presence of quartz silt does not affect the mechanism behind the deflocculation of kaolinite with NaHMP.
- Adding NaHMP into limestone leads to the dissolution of the calcite.
- This dissolution results in an increase of Ca ions concentrations in the pore solution.
- These Ca ions complex with phosphates anions leading to a partial coagulation.
- The delayed flocculation targeted with the addition of magnesium oxide can be compromised by the mechanisms occurring during the former deflocculation.

GRAPHICAL ABSTRACT



ARTICLE INFO

Keywords:

Chemical properties
Rheology
Earth-concrete
Sodium hexametaphosphate
Deflocculation
Coagulation

ABSTRACT

This paper investigates the impact of the chemical composition of two silts, quartz and limestone, on the deflocculation/coagulation process for poured earth application. The driving mechanisms behind the evolution of the rheological behavior after the addition of sodium hexametaphosphate are highlighted through zeta potential measurement and the chemical changes with ICP-OES and ³¹P MAS NMR spectroscopy. The first results show that adding sodium hexametaphosphate into the quartz silt modifies its inter-particle forces through electrostatic repulsion forces induced by the adsorption of phosphate anions onto the quartz structure. For limestone paste, the deflocculation mechanism is affected by the dissolution of the calcite. This dissolution leads to a release of Ca²⁺ cations and an increase in the paste's pH, reducing the paste deflocculation rate. These dissolved Ca²⁺ cations in the solution conduct to a partial coagulation making the delayed flocculation targeted initially with the addition of magnesium oxide less effective.

* Corresponding author.

E-mail address: dardant@ethz.ch (D. Ardant).

<https://doi.org/10.1016/j.colsurfa.2024.134147>

Received 7 March 2024; Received in revised form 23 April 2024; Accepted 30 April 2024

Available online 4 May 2024

0927-7757/© 2024 The Author(s). Published by Elsevier B.V. This is an open access article under the CC BY-NC-ND license (<http://creativecommons.org/licenses/by-nc-nd/4.0/>).

1. Introduction

The construction industry is increasingly adopting earthen construction materials due to their eco-friendly nature [1], their potential for recycling [2], and the high availability of resources for their production [3,4]. Recognizing the similarities between earth and concrete, and applying scientific knowledge gained from the concrete industry can enhance earthen construction practices. A significant advancement in earthen construction is the development of a poured earth technology, which allows for casting fluid earth into hermetically sealed formworks commonly used for construction in poured concrete [5–7]. This innovative technique usually uses Portland-based cement to facilitate the setting since the earth cannot dry within a sealed formwork [8], combined with a superplasticizer to decrease the water-to-binder ratio and the substantial porosity and shrinkage [9].

New attempts were made to remove the cement from the binding fraction through the control of the colloidal state of the dense clay suspension, evolving from a deflocculated state to a coagulated one with the help of additives commonly used in ceramics. The deflocculation of a dense clay suspension improves the workability of the paste by keeping relatively low water to solid ratio. Different deflocculant such as sodium polyacrylate (PAAS) [10], sodium hydroxide (NaOH) [11,12], sodium silicate (NaSi) [12,13], sodium hexametaphosphate (NaHMP) [10, 13–16], or bio-based alternatives such as tannins [11,17], have been successfully tested on dense clay suspension. Their ability to control the edge and face charges of clay particles leads to a change in the clay platelet organization from a house of card structure to an organized one. The coagulation of a clay suspension can be achieved by using an inorganic coagulant such as calcium, magnesium, or sodium minerals acting on the adsorption and the exchange of cations in the clay inter-layer [18].

Based on the mechanism that could be involved in the deflocculation and the coagulation of clay suspension, Landrou et al. suggested to combine both mechanism to control the rheological properties of a clay suspension overtime for a poured earth application. [12,18]. Following this hypothesis, research was done on a dense kaolinite suspension using NaHMP as a deflocculant and magnesium oxide (MgO) as a coagulant to better understand the interactions occurring within the system. The authors suggested that the high effectiveness of NaHMP to deflocculate the kaolinite dense suspension was the direct consequence of the adsorption of the hexametaphosphate anions onto the clay particles' edges, leading to strong electrostatic repulsion forces between the clay particles [13]. They also exposed that the delayed action of MgO as a coagulant leads to the precipitation of the adsorbed hexametaphosphate anions into magnesium phosphate, nullifying their effects on the clay particles edges and bringing then the kaolinite suspension to its initial state [18]. It was also revealed that this process does not modify the clay structure, as the reaction between the additives creates a new mineral component present in such a low quantity that no binding abilities are provided [14,18].

Following the findings on dense kaolinite pastes, this research aims to better understand the established deflocculation/coagulation process on a wider spectrum by adding pure silt to the dense suspension. As the mineral composition of the silt fraction is linked to the weathering process, it can change significantly between different localities. Knowing the remarkable ability of NaHMP to complex with flocculant cations such as Ca^{2+} or Mg^{2+} [19] and the relatively small particle size of silt (below 100 μm , order of magnitude), the mechanism presented for kaolinite paste might be affected by the chemical composition of the silt. There is no consensus in the literature regarding the interaction between sodium hexametaphosphate and the silt fraction. Liang et al. [20] suggest that adding NaHMP in diluted quartz modifies the Van der Waals interactions and the electrostatic double layers forces, which can influence the paste yield stress. In opposition, Kohandelnia et al. [21,22] show that NaHMP does not act on the yield stress of quartz paste. Moreover, there is a lack of literature regarding the delayed flocculation

of deflocculated pastes containing silt in the binding paste, as literature focuses only on the mechanism involved in kaolinite-rich suspensions [14,18]. It can be suggested that if the silt stability might be affected by NaHMP, some flocculant ions might precipitate with the hexametaphosphate anions. Hence it might reduce the amount adsorbed onto the clay particles' edges affecting the precipitation of these anions with MgO. Therefore, this research focuses on two silts with different chemical compositions, quartz (SiO_2) and limestone (CaCO_3). Their interaction with NaHMP as deflocculant will be examined, and the entire deflocculation/coagulation process will be analyzed on binary mixes with kaolinite.

2. Materials

2.1. Silts

Two fine mineral powders (mineral flours) with distinct mineralogical compositions were selected for the experimental investigation to mimic the silt fraction. The first "silt" is a pure quartz flour ($\text{SiO}_2 > 97 \text{ wt } \%$), sourced from Bernasconi AG (Switzerland), with a maximum particle size of 63 μm , a D10 of 0.15 μm and a D50 of 5.83 μm . The second one is a high-purity limestone flour ($\text{CaCO}_3 > 96 \text{ wt } \%$) also sourced from Bernasconi AG (Switzerland). Initially, the limestone flour was received with a maximum particle size of 200 μm , and to ensure consistency, it was sieved to isolate the fraction below 63 μm and keep a constant with the quartz silt. Its D10 is 1 μm , and its D50 is 7.03 μm . The particle size distribution of the two silts studied was measured using an automatic sedimentometer (PARIO Meter, Germany) following the norm ISO 11244:2020 [23]. The particle size distributions of the two silts are gathered in Fig. 1.

2.2. Clay

Experiments on binary mixes were carried out on clay-silt mixes using a kaolinite powder as the clay mineral fraction. The kaolinite chosen is a commercial clay for ceramic application referred to here as Kaolinite FP80 and sourced from Dorfner (Germany). It has a maximal particle size of 51 μm , a D10 of 1.78 μm , and a D50 of 3.06 μm . Its mineralogical composition was investigated by XRD using a Bragg-Brentano X-ray diffractometer (D8 Advance, Bruker, AXS, Germany) with Cok radiation. The kaolinite powder was milled with isopropanol in a McCrone Micronising mill to pass through a 20 μm sieve and, after drying at 65 $^\circ\text{C}$, put directly into the sample holder with the help of a razor blade to avoid the preferred orientation. The analysis of the qualitative phases was carried out with the software DiffraCeva using the PDF-2 database from the International Center for Diffraction Data. The qualitative analysis was performed using the Rietveld method [24] with the software Profex [25]. Results revealed that kaolinite is the main component, but not the only one. The powder cannot be considered pure kaolinite as the amount of accessory minerals (12.8 %) is relatively high. The whole chemical composition of the powder is gathered in Table 1.

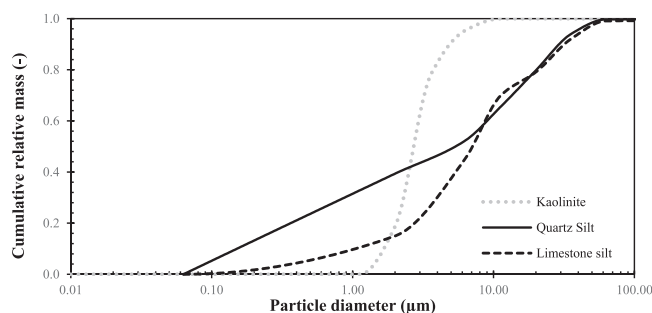


Fig. 1. Particle size distribution of the two silt powders and the kaolinite used in this research.

Table 1

Chemical composition of the kaolinite studied by quantitative X-ray diffraction analysis. Values are given in wt %.

Kaolinite	Quartz	Muscovite	Microcline	Anhydrite
87.2	4.0	3.6	3.6	1.6

2.3. Additives

Two additives already explored for adjuvanted earth-concrete [14, 18] were used. The first one, a high purity sodium hexametaphosphate ($\text{NaPO}_3)_6$ (>99 wt % pure) in powder form sourced from Sigma Aldrich (Switzerland), is used as deflocculant (referred to here as NaHMP). A NaHMP solution is prepared at a dilution rate of 10 wt % in deionized water. The second one, a high-purity magnesium oxide (MgO , >97 wt % pure) sourced from Sigma Aldrich (Switzerland), is used as a coagulant.

3. Experimental procedure

3.1. Rheology measurement

3.1.1. Paste preparation

Rheology measurements were performed on different pastes composed of pure silt, binary mixes of silt-kaolinite, and pure kaolinite. The aim was to study the effect of the additives on the rheological properties of the suspension directly after mixing and their stability over time. Even if the particle size distribution of the two silts differed, the water-to-solid (W/S) ratio used for their pastes was kept constant at 0.255 to facilitate the comparison. This ratio was defined to get pastes with a solid volume fraction relatively close to their dense solid volume fraction. This ratio was updated to 0.50 for binary silt-kaolinite mixes and 1 for pure kaolinite paste. Only the dosage of the deflocculant and the coagulant were varied from one sample to another. The dosages in NaHMP are always expressed as the percentage of the mass of solid content. The dosages of MgO are expressed as a magnesium-to-phosphate molar ratio (Mg/P).

The preparation procedure for the different mixes is synthesized as follows. Initially, the powders were manually homogenized, and the diluted NaHMP solution was incorporated into water. The powders and the liquid were mixed for 2 minutes at 365 rpm using a mechanical stirrer equipped with a four-bladed mixing tool (Heidolph Instrument, Switzerland). In the case of measurements involving the addition of coagulant, MgO powder was added, and the paste was mixed again for 2 minutes at 365 rpm. All the samples are prepared at room temperature ($23 \pm 1^\circ\text{C}$).

3.1.2. Flow onset measurements

Flow onset measurements were performed for the yield stress measurements of the different pastes after introducing NaHMP. The rheological measurements were performed using a Malvern Kinexus Lab + (Malvern Instruments, Switzerland) stress-controlled rheometer equipped with serrated parallel plates of a diameter of 40 mm to prevent slip at the shearing surface [26]. The lower plate was filled with the sample directly after the mixing phase. Then, the upper plate was placed with a gap of 2 mm between the plates to ensure a minimum spacing exceeding the largest particle size by a factor higher than ten [27]. The sample was finally covered with a trap cover to minimize evaporation during the measurement. After 1 min resting time, a constant shear rate of 0.01 s^{-1} was applied to the sample for 240 s. At such a low shear rate, the influence of the viscosity on the measurement is negligible, allowing the computation of the yield stress from the measured torque peak value at the onset of flow [27,28]. The whole protocol was repeated three times for each mixture to enhance accuracy.

3.1.3. Dynamic yield stress measurement overtime

The influence of the pastes' composition on the deflocculation effect

of NaHMP over time was studied through two binary mixes (kaolinite-quartz and kaolinite-limestone) prepared at their optimal dosage of NaHMP. The stress-controlled rheometer was equipped with a Vane geometry to avoid the potential drying with serrated plates after hours of resting time. The Vane geometry consists of a four-bladed paddle with a diameter of 25 mm, and the outer cup diameter is 25 mm with a depth of 63 mm. Using a 4-bladed paddle minimizes the material's disturbance during the introduction of the vane and avoids the wall slip effect [29]. After filling the cup, the vane was inserted, and a trap cover was added to minimize evaporation. The paste was left one minute undisturbed before starting the measurement. The measuring sequence included the following steps: an increasing shear rate ramp from 0.1 s^{-1} to 300 s^{-1} (with a logarithmic distribution of shear rates) was applied during 300 s, followed by a decreasing shear rate ramp from 300 s^{-1} to 0.1 s^{-1} during 300 s. The procedures were done after six resting times (directly after mixing and after the resting time of 30 min, 1 h, 2 h, 4 h, and 6 h). The yield stress value was extrapolated at low shear rates through a linear regression according to the Herschel-Bulkley model with $\tau = \tau_0 + \eta_{HB}\dot{\gamma}^n$, where τ is the shear stress, τ_0 is the yield stress, $\dot{\gamma}$ is the shear stress, η_{HB} is the consistency index, and n is the flow index [26]. Only the decreasing ramps were studied to get yield stress values after a stress allowed to break the particle network built during the resting time, giving a better view of the aging phenomenon.

3.2. Zeta potential

The measurement of ζ -potential was performed using a ZetaProbe instrument (Colloidal Dynamics, Ponte Vedra Beach, FL, USA) employing the electro-acoustic method. This technique involves the application of a high-frequency alternating electric field, causing charged particles to oscillate. The motion of these particles generates a sound wave, which is captured and provides information about the dynamic mobility of the particles [30]. The experiments to determine ζ -potential were conducted on suspensions of pure silt. The solid volume fraction corresponding to the suspension in deionized water was approximately equal to 48.9 vol %. To mitigate issues related to sedimentation and prevent measurement artifacts, blade stirring at 365 rpm was employed during the measurement. The dosages of dispersant used in these experiments were maintained at similar levels concerning the silt content as those employed in the rheological measurements.

3.3. Solid-state ^{31}P magic angle spinning nuclear magnetic resonance (MAS NMR)

^{31}P MAS NMR was performed on chosen pastes. These pastes are binary silt-kaolinite pastes (kaolinite-limestone and kaolinite-quartz) with a W/S ratio of 0.5 and an amount of NaHMP fixed at 0.2 wt% by solid. After mixing, each paste was split in two. One part was sealed for 4 hours and dried overnight at room temperature ($23 \pm 1^\circ\text{C}$). Magnesium oxide was added in the other part, in a proportion leading to a phosphate-to-magnesium molar ratio of 16. This part was mixed again for 2 min, sealed for 24 hours, and dried overnight at room temperature ($23 \pm 1^\circ\text{C}$). The four dried samples were then crushed using agate mortar. The ^{31}P MAS NMR data were acquired using a 4 mm rotor at rotation rates of 10,000 Hz at 162.0 MHz as single pulse experiments with $2.0\text{ }\mu\text{s}$ (40°) excitation pulses, 58 kHz SPINAL 64 proton decoupling was applied during acquisition, and the recycle times of 10 s ensured quantitative acquisition of the spectra. ^{31}P NMR chemical shifts were referenced to the external standard of $\text{NH}_4\text{H}_2\text{PO}_4$ (solid) at 0.0 ppm.

3.4. Solid/liquid phase separation and solution analysis

The sample preparation and the measurement procedure for inductively coupled plasma – optical emission spectrometry (ICP-OES), pH, and total dissolved inorganic carbon (TDIC) measurements were

performed as follows. The pastes were prepared according to the procedure outlined in Section 3.1.1 to obtain pore solutions for solution analysis. Subsequently, the pastes were transferred to 50 mL centrifuge tubes and left undisturbed for 24 hours with the lids closed to allow the reaction to occur. After resting, the samples were vortexed and centrifuged at 4000 rpm for 10 minutes. This process separated the pore water from the solid, which was then transferred to 15 mL centrifuge tubes. The centrifugation step was repeated twice more at 4000 rpm for 10 minutes.

The resulting pore solution was filtered using an MN615 filter and a Whatman cellulose filter with a pore size of 0.45 μm . The filtered solution was stored at ambient temperature before being subjected to measurement and diluted with nitric acid (prepared from Merck HNO_3 suprapur quality, 65 %, with high-purity water (18.2 $\text{M}\Omega/\text{cm}$, Millipore) on the day of the measurement. The measurements were repeated three times under the same conditions. The concentration of sodium [Na], phosphorous [P], aluminium [Al], silicon [Si], magnesium [Mg], calcium [Ca], iron [Fe], potassium [K], and sulfur [S] was measured by ICP-OES (Agilent 5110 ICP-OES).

The measurement of the total dissolved inorganic carbon was carried out with TOC analyzer Sievers 5310 C, connected to a Sievers 900 autosampler station. Filtered samples were diluted to 1:30 with ultra-pure water for analysis. Finally, pH measurements were conducted on the unfiltered aliquots using a Thermo Scientific™ Orion™ Per- pHecT^{TM} ROSS™ Combination pH Micro Electrode.

4. Results and discussion

4.1. Deflocculation mechanism of silt fraction

Fig. 2 shows the sensitivity of the silts to the NaHMP. Quartz silt displays a higher sensitivity to the deflocculant than limestone silt. The value of the lowest yield stress reached after deflocculant addition is also higher for limestone paste than for quartz. Subsequently, in both cases, after reaching the optimum amount, the yield stress increases, indicating the displacement of the saturation point, also exposed in literature when NaHMP is used to deflocculate clay-rich minerals [10,13].

Hence, the silt powders' mineralogical composition drastically influences the dosage of NaHMP to target the highest change in paste behavior. The literature has exposed similar observations on kaolinite, whether pure or with accessory minerals [19]. The authors exposed that the NaHMP amount needed to reach the paste's lowest viscosity value was much higher for the kaolinite containing the accessory minerals, even if the specific surface area of both powders was relatively close.

Following this observation on rheology measurement, zeta potential was conducted to better understand the evolution of the two quartz and limestone silt surface charges over the addition of NaHMP. (Fig. 3)

In the case of quartz, the pH decreases with a small NaHMP addition

from 8 to 7. A constant pH at 7 is visible when 0.015 wt % of NaHMP is reached. The zeta potential also decreases values, from -45 mV initially to a plateau at -60 mV, obtained at an amount of NaHMP around 0.015 wt %. For limestone, the addition of NaHMP results instead in an increase in pH of the suspension, from 8 and leveling off around 10 at 0.04 wt % of NaHMP. The zeta potential, initially positive, drastically decreases to -30 and -50 mV, for 0.02 and 0.06 wt % NaHMP added, respectively. For both silts, adding NaHMP results in negative particle surface charges.

The yield stress of colloidal systems is influenced by the nature and strength of inter-particle forces, which can be influenced by several factors such as pH, ionic strength, or adsorbed molecules [11]. Furthermore, it has been verified that deflocculants can modify inter-particle forces by enhancing them through repulsive electrostatic and/or steric forces [11]. This action ultimately results in the deflocculation of colloidal particles, affecting the macroscopic yield stress of the material.

The nature of interaction forces can be characterized using the DLVO theory [31,32], which establishes a relationship between the yield stress and zeta potential through the following equation.

$$\tau_0 = \frac{3\phi^2}{2\pi a} \left(\frac{A_0}{48\pi d_0^2} - B\zeta^2 \right) \quad (1)$$

$$\text{with } B = \frac{K\kappa}{4\pi} (1 - \tanh(\kappa d_0)) \quad (2)$$

Where τ_0 is the yield stress, ϕ the solid volume fraction, a the radius of particles, A_0 the van der Waals constant, d_0 the interparticle distance, ζ the zeta potential of suspension, K the permittivity of free space, and the area of interaction is assumed to be given by πa^2 , and κ the Debye parameter.

A clear relationship between the yield stress and the squared zeta potential at a given solid volume fraction indicates the presence of electrostatic repulsion forces between particles [33]. Looking at Fig. 4, electrostatic repulsion forces are the only modification in inter-particle forces observed after the NaHMP addition in quartz silt paste. Knowing that the quartz used here is exceptionally pure ($\text{SiO}_2 > 97$ wt %) and that its structure is known as stable in the condition used here, as exposed by its initial zeta potential value, it could be suggested that the increase in repulsive forces is guided in prior by the adsorption of phosphate anions on the surface of the quartz particle, as exposed in [20].

In contrast, there is no linear correlation between the yield stress and the squared zeta potential for limestone silt. The positive zeta potential value before NaHMP addition suggests unstable colloids with interaction dissolving with a slight modification of the environment. The introduction of NaHMP leads to a partial dissolution of the silt and complexation with calcium [19] can change the colloid interaction, as seen with the sudden increase in pH value. This evolution to basic pH can increase the dissolution process of calcite, leading to more calcium and carbonates in the solution [34]. Additionally, Ca cations can form with hexametaphosphate (HMP) anions, a strong 1:1 outer-sphere complex with a high stability constant [35]. Hence, the combining effect of (i) the increase in repulsive forces, (ii) the dissolution of calcite, and (iii) the strong complexation of the flocculant Ca cations with phosphate anions, potentially (iv) the formation of Ca-phosphate solids could explain the results observed in Fig. 2. Those four hypotheses need to be confirmed.

Regarding the results obtained in this section, it can be stated that NaHMP can deflocculate silt pastes. However, its mineralogical composition drastically influences the mechanisms behind this deflocculation. As silt paste will never be used without a clay fraction as a binder for earthen components, it is thus necessary to have a better look at the deflocculation and the coagulation process developed on deflocculated paste on binary clay-silt pastes.

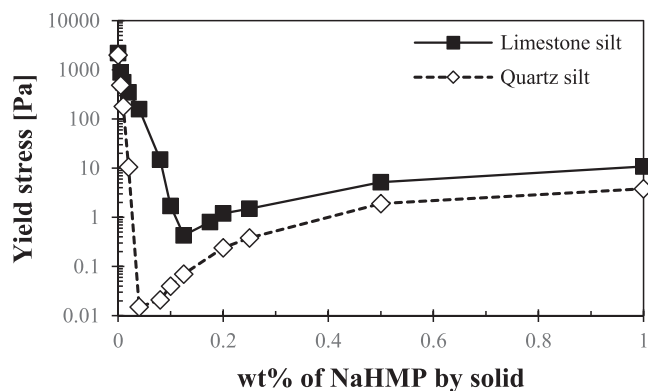


Fig. 2. Effect of NaHMP on the yield stress of silt pastes at constant water content (25.5 wt %).

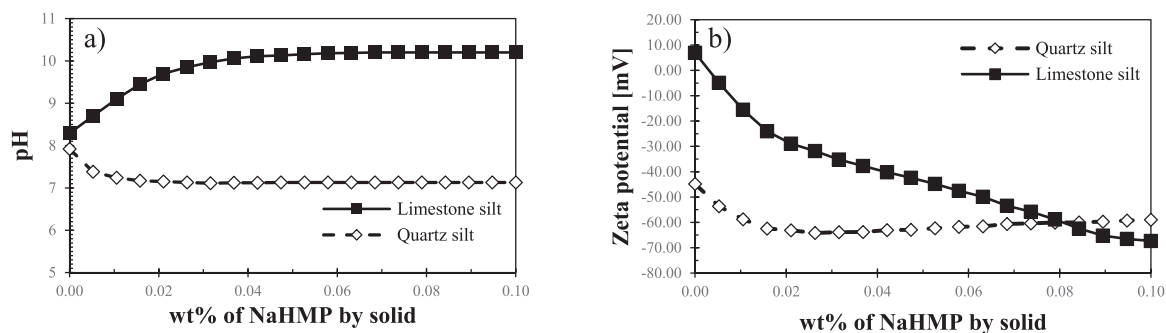


Fig. 3. Evolution of silt pastes pH (a) and zeta potential (b) after addition of NaHMP.

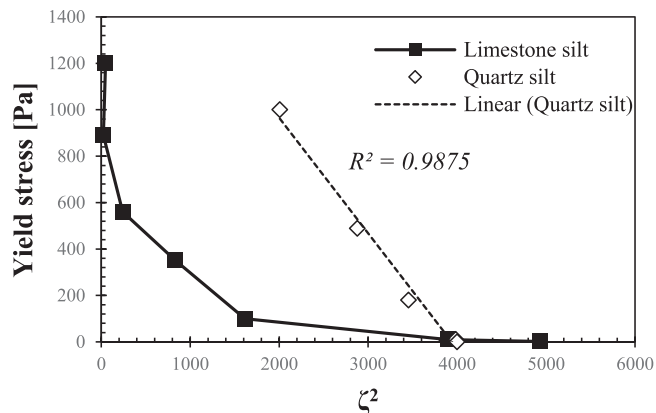


Fig. 4. Relationship between the yield stress and the square zeta potential of studied pastes prepared with NaHMP.

4.2. Deflocculation/Coagulation mechanism of binary mixes with kaolinite and silt

4.2.1. Effect of deflocculant on the rheological behavior

At first, similar rheological measurements are performed on the new binary mixes and the pure kaolinite as a reference (Fig. 5).

It can be noticed that the addition of kaolinite in the silt mixtures provides better control over the NaHMP addition. Adding NaHMP to binary pastes does not result in similar yield stress evolution, indicating again that the silt's mineralogical composition influences the NaHMP's action.

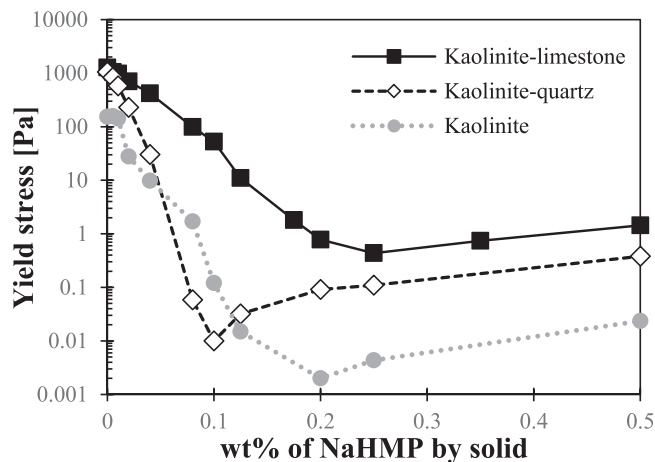


Fig. 5. Effect of NaHMP amount on the yield stress of quartz-kaolinite mix and limestone-kaolinite mix with the same water-to-fine ratio (0.5) and on the yield stress of kaolinite with a water-to-solid ratio of 1.

For kaolinite-quartz binary mixes, the NaHMP needed to reach the lowest yield stress value is around 0.1 wt %. It corresponds to half of the amount needed to reach the lowest value for kaolinite paste (0.2 wt %). These results and the fact that binary mixes contain 50 % kaolinite suggest that the quartz silt does not adsorb HMP anions and does not influence the binary paste deflocculation mechanism. It can be the consequence of the good stability of the quartz structure [20,36]. Consequently, the evolution of the yield stress value might be related to (i) the increase of the negative charge on the clay micelles through the adsorption of phosphate anions, (ii) the complexation of the flocculant cations in the kaolinite and its accessory minerals, and (iii) the substitution of the cations in double clay layer with Na ions [19]. As these three mechanisms are known to be more efficient at either low or high NaHMP, the optimal amount seen here can be the intermediate concentration, leading to their best synergy [19].

The kaolinite-limestone mix requires nearly the same amount of deflocculant as kaolinite paste to reach its lowest yield stress (0.25 wt %), indicating that limestone reduces deflocculant capacities of NaHMP on kaolinite. Andreola et al. [19] have also exposed a reduction of NaHMP efficiency for kaolinite paste containing accessory minerals, thanks to the dissolution of the calcium and magnesium compounds in presence of NaHMP. In the case of kaolinite-limestone, if the NaHMP addition leads to the dissolution of calcite, the Ca^{2+} cations in the paste can induce this reduction. If Ca^{2+} cations are present, an aging phenomenon on the paste yield stress might be visible [12,37].

Looking at Fig. 6, the two pastes recover their initial behavior after stress, allowing the rupture of the particle network interactions. For kaolinite-quartz paste, the behavior is identical after the different resting times (Fig. 6a). These observations are in line with the literature on kaolinite paste, exposing the same behavior over time when NaHMP is added (i.e., reversible behavior) even if Ca^{2+} or Mg^{2+} cations are present from the accessory minerals [13,37]. The limestone binary paste exhibits a slight increase in yield stress over time, displaying an aging phenomenon (Fig. 6b) and suggesting the presence of Ca^{2+} cations from the calcite dissolution.

When NaHMP is mixed with lime, the released Ca^{2+} cations precipitate with phosphate anions, forming hydroxyapatite ($\text{Ca}_{10}(\text{PO}_4)_6(\text{OH})$) at least 3 hours after mixing [12]. In this study, this precipitation cannot be confirmed as no hydroxyapatite, (~ 2 ppm) [38], can be observed in the kaolinite-limestone paste 4 hours after mixing (Fig. 7). The ^{31}P MAS NMR data of the deflocculated kaolinite-quartz and the kaolinite-limestone pastes presents two main signals. The signal at -21 ppm can be attributed to a Q^2 polyphosphate species, exposing the remaining phosphate cycles associated with NaHMP [39]. The other main signal at approximately -6 ppm can be attributed to hydrogen phosphate or pyrophosphate, which could indicate phosphate adsorption on the clay micelle [40,41]. By the end, the slight aging phenomenon observed for a 4-hour resting time in Fig. 6b can result from the adsorption of Ca^{2+} cations in the Stern layer of kaolinite, which effectively reduces the electrophoretic mobility of its particles over time [37].

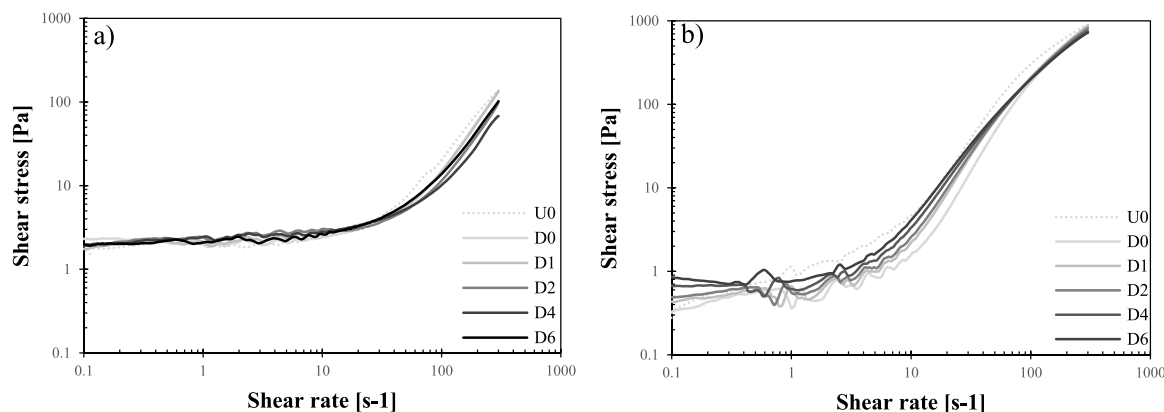


Fig. 6. Flow curve measurements at different acquisition times for quartz-kaolinite paste with 0.1 % NaHMP (a) and for limestone-kaolinite paste with 0.2 % NaHMP (b) (U represents ramp up during the sequence, and D represents ramp down. The number indicates the acquisition time in hour).

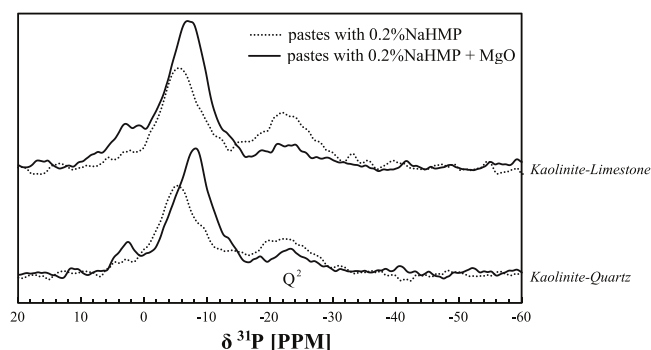


Fig. 7. ^{31}P MAS NMR spectra of kaolinite-quartz and kaolinite-limestone pastes 4 hours after being deflocculated with 0.2 %NaHMP and 24 hours after the addition of MgO ($\text{Mg}/\text{P}=16$) in the deflocculated pastes.

Magnesium oxide added into a deflocculated paste with NaHMP has been used to stop the activity of NaHMP by precipitating phosphate anions with Mg^{2+} cations [18]. The consequence of this addition is a drastic increase in the paste yield stress value after a specific resting time. The resting time of 24 hours is given as a reference as it corresponds to the time needed to bring a kaolinite paste back to its initial state when it is prepared at its optimal NaHMP amount [18].

As a general observation for the three types of paste tested here, increasing the Mg/P ratio always increases the paste yield stress (Fig. 8), as exposed in the literature [18].

Kaolinite-quartz paste follows a yield stress evolution close to that of kaolinite paste. These dispersed pastes return almost to their initial state when a Mg/P molar ratio equal to 16 is reached. These results exposed

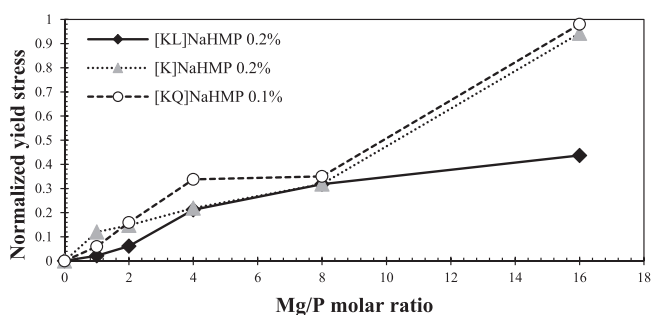


Fig. 8. Evolution of the yield stress measured after 24 h as a function of the molar ratio Mg/P for different mixtures. To facilitate the comparison between the pastes, the yield stress value has been normalized by the yield stress of the paste prepared without additives.

that quartz is not involved in the mechanism leading to the coagulation of the paste. Consequently, the coagulation is completed for the kaolinite-quartz paste when the precipitation exposed to the kaolinite paste has been completed. The mechanism for the limestone binary mix is diminished. Looking at the values, a plateau starts to appear slightly at a Mg/P ratio of 8, meaning that an increase in the Mg/P molar ratio would not have been conducted to bring the paste back to its initial yield stress.

Following the results obtained for a resting time of 24 hours, the two pastes show a difference in the early aging process (Fig. 9). The kaolinite-quartz (Fig. 9a) structures quickly with a high change in the yield stress values after one hour of resting. At 6 hours, the paste keeps increasing its yield stress value. In contrast, the kaolinite-limestone paste (Fig. 9b) has slow structuration over time. The values seem to stagnate after 4 hours of resting.

This observation at early aging confirms the influence of the silt composition on the coagulation mechanism during the early structuration. In the literature, it has been exposed that adding MgO powder into deflocculated kaolinite paste leads to a homogeneous flocculation that creates new precipitate phases [18]. This precipitation can be suggested by looking at the change occurring in the ^{31}P MAS NMR spectra for the samples prepared with MgO and left undisturbed for 24 hours. The Q^2 signal at -21 ppm is decreased, suggesting fewer phosphate cycles associated with NaHMP. The signal at -6 ppm is less visible, and new peaks can be observed at approximately -8.5 ppm and 3 ppm. It has been strongly suggested that these two peaks could be related to new poorly crystalline phosphate-containing phases similar to newberyite ($\text{MgHPO}_4 \cdot 3\text{H}_2\text{O}$), for the signal at 3 ppm, and similar to bobierrite ($\text{Mg}_3(\text{PO}_4)_2 \cdot 8\text{H}_2\text{O}$), for the one at -8.5 ppm [40].

For the kaolinite-limestone samples, a slight peak around 2 ppm exists, suggesting, by the end, the presence of hydroxyapatite related to the dissolution of the calcite exposed previously [42]. However, it remains unclear for now if the addition of MgO increases the precipitation between HMP anions and Ca^{2+} cations or if it occurs after 4 h resting. A closer look at the pH evolution and the ions released in the different pastes can help to get a better understanding.

This difference between the structuration can result from a change in the coagulation process: incorporation of cations in the clay interlayers for dissolved calcium ions and homogeneous flocculation for magnesium ions dissolved later in a deflocculated paste. This supposition is strengthened by the low solubility of MgO, leading to a delayed release of ions compared to calcite [14].

4.2.2. Ions released

To complete the rheology measurements and confirm the mechanisms and the reactions highlighted in this former section, the pore solution of the three pastes mixed with different NaHMP dosages after 24 h

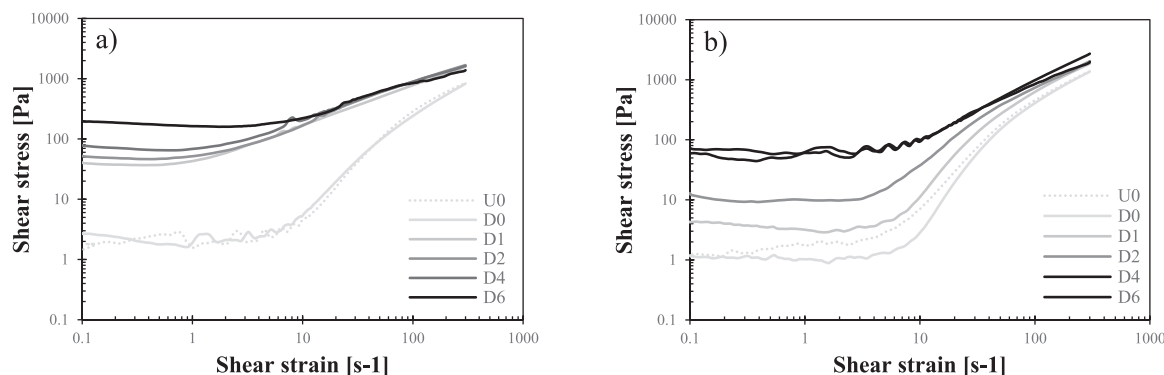


Fig. 9. Flow curve measurements at different acquisition times for quartz-kaolinite paste with 0.1 wt % NaHMP (a) and for limestone-kaolinite paste with 0.2 wt % NaHMP (b) after the addition of MgO (Mg/P molar ratio of 16) (U represents ramp up during the sequence and D represents ramp down. The number indicates the acquisition time in hour).

resting time was analyzed. Data are shown in Fig. 10 and Table 2. As kaolinite paste is prepared with different water content, the amount of NaHMP in the pore solution is presented in concentration (mmol.L^{-1}) to facilitate the comparison of the results. In Fig. 10, the P and Na ions concentrations in the pore solution for the three pastes are plotted as a function of the NaHMP concentration.

For all pastes, the concentration of Na increases similarly through the NaHMP addition. It confirms that the silt mineralogy does not affect the uptake of sodium by the solids. This disappearance seems only related to the kaolinite fraction through (i) the cation exchange process with flocculants cations, (ii) the co-adsorption with phosphate anions and, possibly, (iii) the reprecipitation with Al and Si into Na-smectite [13,19,37,43]. The presence of flocculant ions in the pore solution (Table 2) can be related to the replacement by Na ions through the cation exchange. The other phenomena cannot be confirmed in the present research.

Looking at the P ions in the pore solution, kaolinite and kaolinite-quartz mixes exhibit similar concentrations. The results are in accordance with the ones observed during the rheological measurements. It can be confirmed that for these two pastes, the disappearance of the P ions is the consequence of the phosphate anion adsorption on the clay micelle [19].

For the limestone binary paste, the higher pH and the presence of inorganic carbon in the kaolinite-limestone paste (Table 2) validate the

dissolution of calcite. The high amount of Ca ions in the pore solution of the paste containing limestone can be explained by this dissolution. The remaining presence of Ca and P ions after 24 h hours of resting could be linked to the strong 1:1 complexation between Ca^{2+} cations and phosphate.

Its lower concentration of P ions compared with the two other pastes can consequently result from several mechanisms following this dissolution. It can be due to (i) the interaction between Ca^{2+} cations from the dissolution of the calcite and phosphate anions [35] and/or (ii) the increase of pH in the solution, leading to deprotonation of the kaolinite, hence higher sorption of the phosphate [44]. The amount of Ca ions is relatively close to the one in the pore solution of kaolinite quartz mixes, which seems to confirm the precipitation suggested previously between HMP anions and Ca^{2+} cations. It seems in the end that hydroxyapatite formation occurs even without adding MgO but after a higher resting time than the one exposed in the literature [12].

In the former section, it has been suggested that the addition of magnesium oxide in the different pastes deflocculated with NaHMP leads to a precipitation of the phosphate compounds adsorbs on the clay micelle and the remaining polyphosphates associated with the NaHMP with the magnesia introduced. The concentration of the ions in the pore solution can give input on these new precipitates. For a better view of the influence of the MgO concentration in the different pastes, two Mg/P ratios are tested: 2 and 16.

Fig. 11 shows that through the Mg/P molar ratio increases, the P ions in the pore solution drastically decrease for all pastes, leading to values below 1.2 mmol.L^{-1} at a Mg/P molar ratio of 16. As the amount of Mg ions introduced initially also drastically decreases after 24 hours (Table 3), it can be confirmed that precipitation between phosphate and magnesium occurs during this resting time, as exposed in [18,40] and suggested by the results obtained in Fig. 7. The precipitation can be strengthened by the drastic increase of all pastes pH when MgO is introduced in the system, improving the precipitation. This improvement can also explain the decrease in Ca ions in the pore solution by precipitation into poorly-crystalline hydroxyapatite, as observed in Fig. 7 on kaolinite-limestone samples 24 h after adding MgO. The amount of Na ions in the pore solution remains almost constant for all pastes. It exposes that the MgO introduction does not affect mechanisms related to the Na disappearance after the NaHMP addition.

The amount of Si and Al in solution does not drastically decrease, in opposition with what has been exposed in [18], and the precipitation of Al and Si with Mg ions into magnesium alumina silicate and magnesium alumina cannot be confirmed here. As the change in pH can also increase the deprotonation of kaolinite, the increase in pH observed in Table 3 can lead to the differences observed for these ions.

Unlike their rheological measurement obtained in the former section, the pore solution analysis does not exhibit drastic differences between the three pastes studied. The consumption of P ions from the pore

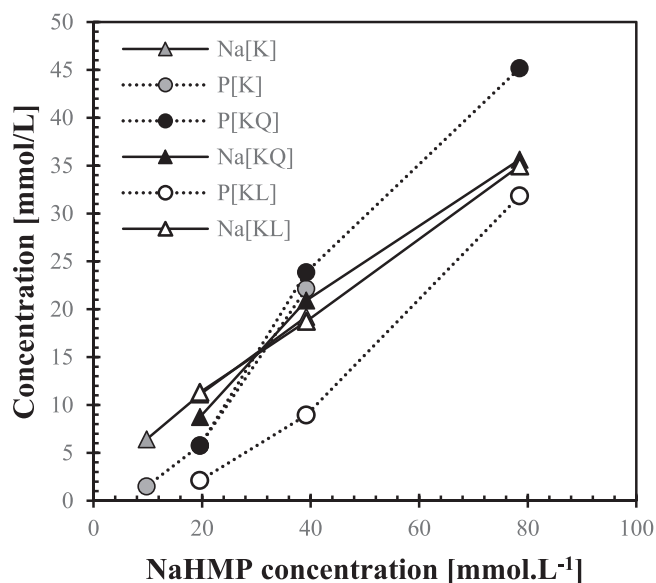


Fig. 10. Concentration in mmol.L^{-1} of P and Na ions in pore solution for the three pastes tested at different NaHMP concentrations.

Table 2
Concentration of a collection of cations after 24 h of contact between kaolinite(K), kaolinite-quartz (KQ), kaolinite-limestone (KL), and NaHMP solution as a function of a starting concentration of NaHMP (NaHMP C.). b.d.l.= below detection limit.

Mix	NaHMP C. [g.mL ⁻¹]	NaHMP C. [mmol.L ⁻¹]	P [mmol. L ⁻¹]	Na [mmol. L ⁻¹]	Si [mmol. L ⁻¹]	Al [mmol. L ⁻¹]	Ca [mmol. L ⁻¹]	Mg [mmol. L ⁻¹]	S [mmol. L ⁻¹]	Fe [mmol. L ⁻¹]	K [mmol. L ⁻¹]	inorganic C [mmol.L ⁻¹]	pH (22° C)
K	0.001	9.8	1.5	6.42	1.2	0.65	0.27	0.2	2.96	0.04	0.21	<0.0007	5.7
K	0.002	19.6	5.78	11.08	2.36	2	0.37	1.13	3.07	0.16	0.50	<0.0007	5.8
K	0.004	39.2	22.13	19.21	3.4	3.94	2.27	0.94	2.98	0.47	0.54	<0.0007	5.7
KQ	0.002	19.6	5.73	8.74	1.89	1.52	0.44	0.25	2.76	0.13	0.36	<0.0007	5.6
KQ	0.004	39.2	23.86	20.92	2.24	2.58	2.82	1.44	3.24	0.34	0.39	<0.0007	5.7
KQ	0.008	78.5	45.17	35.62	1.09	2.6	4.4	1.69	2.61	0.61	0.40	<0.0007	5.7
KL	0.002	19.6	2.11	11.32	1.09	b.d.l	1.15	0.34	2.75	b.d.l	0.20	0.008	7.6
KL	0.004	39.2	8.93	18.73	0.37	b.d.l	2.25	0.55	2.63	b.d.l	0.18	0.008	7.8
KL	0.008	78.5	31.83	34.97	0.37	0.06	7.5	1.1	2.45	b.d.l	0.18	0.007	7.9

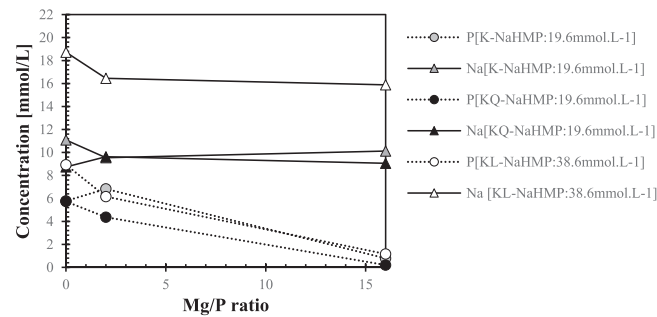


Fig. 11. Concentration of Na and P ions in pore solution after adding MgO at several Mg/P ratios.

solution cannot always be related to the complete annihilation of the NaHMP activity on the paste. The fact that the kaolinite-limestone paste cannot reach a yield stress value equivalent to its initial one after MgO addition might result from the mechanisms highlighted during the deflocculation step. The coagulation resulting in the calcite’s direct dissolution into Ca²⁺ cations and their complexation and precipitation with phosphate anions [37] affect the homogeneous flocculation obtained by incorporating MgO into the deflocculated paste.

5. Conclusion

Controlling the rheological behavior of a rich clay paste through the deflocculation/coagulation process can be a promising strategy for developing earth-concrete. However, this mechanism needs to be fully apprehended, as previous research only explored the mechanism in depth on kaolinite paste. The chemical composition of other compounds present in earth fine fractions, such as quartz or calcite, might interact with the mechanisms highlighted for kaolinite-dense suspension. The results showed that the pastes based on kaolinite and distinct silt with different mineral compositions (quartz (with the chemistry SiO₂) and

limestone (with the chemistry CaCO₃)) were not deflocculated and coagulated as the pure kaolinite. In particular, NaHMP was less efficient for the mix containing limestone.

The driving mechanism behind the deflocculation of the silt particles with sodium hexametaphosphate (NaHMP) is correlated to their chemical composition. Adding NaHMP into quartz silt leads to a modification of its inter-particle forces through electrostatic repulsion forces induced by the adsorption of phosphate anions onto the quartz structure. For limestone paste, the deflocculation mechanism is limited by the partial dissolution of the calcite, leading to a competition of the two mechanism. NaHMP dissolves the calcite resulting in an increase in pH, and an increase of Ca ion concentration in the pore solution. The high complexation Ca-phosphate seems to agree with the higher amount of NaHMP needed to deflocculate the paste with limestone silt and indicates that the phosphate anions are bonding in prior with the released Ca²⁺ ions instead of being adsorbed onto the kaolinite platelets’ edges. In contrast, the quartz, thanks to its stable structure with a neutral surface has little effects, leads to the prior adsorption of HMP anions by the kaolinite micelle.

The pore solution analysis 24 hours after introducing magnesium oxide (MgO) as a coagulant leads to similar results regarding phosphate and magnesium ions concentration between the pastes. It confirms the precipitation of the phosphate adsorbed on the clay micelles into new mineral phases with magnesium compounds, as supposed with the ³¹P MAS NMR spectra obtained for these pastes. This precipitation affects the clay platelets’ organization, leading to increased yield stress values, as observed with the rheological measurements. For kaolinite and kaolinite-quartz pastes, a correlation between the total consumption of P ions and the complete annihilation of the NaHMP effect on the paste yield stress can be seen. However, for kaolinite-limestone, no relation between these two parameters can be established as the paste still displays relatively low yield stress when all P ions have precipitated. The coagulation suggested by the precipitation of phosphate anions and Ca²⁺ cations reduces the delayed homogeneous flocculation obtained after the addition of low soluble MgO.

Table 3
Concentration of a collection of cations after 24 h of contact between kaolinite(K), kaolinite-quartz (KQ), kaolinite-limestone (KL) with their optimal amount of NaHMP and different amounts of MgO, as a function of the Mg/P molar ratio. b.d.l.= below the detection limit.

Mix	NaHMP C. in mmol.L-1	Mg/p [molar ratio]	Mg initial C. [mmol.L-1]	P [mmol. L-1]	Na [mmol.L- 1]	Si [mmol.L- 1]	Al [mmol.L- 1]	Ca [mmol.L- 1]	Mg [mmol.L- 1]	S [mmol. L-1]	Fe [mmol.L- 1]	K [mmol. L-1]	pH (22° C)
K	19.6	0	0	5.78	11.08	2.36	2	0.37	1.13	3.07	0.16	0.50	5.7
K	19.6	2	14.88	6.83	9.54	1.51	1.63	0.47	0.28	2.83	0.15	b.d.l	9.12
K	19.6	16	122.1	0.78	10.12	4.93	3.22	0.06	0.63	3.33	0.20	b.d.l	11.39
KQ	19.6	0	0	5.73	8.74	1.89	1.52	0.45	0.25	2.76	0.13	0.36	5.7
KQ	19.6	2	14.88	4.36	9.63	7.94	0.05	0.3	1.74	2.79	0.32	b.d.l	9.29
KQ	19.6	16	122.1	0.2	9.06	0.37	0.05	0.1	0.04	3.18	b.d.l	b.d.l	11.34
KL	39.2	0	0	8.93	18.73	0.37	0	2.25	0.55	2.63	b.d.l	0.18	7.75
KL	39.2	2	33.36	6.16	16.45	1.48	0.7	0.25	1.62	2.82	0.05	b.d.l	10.32
KL	39.2	16	244.2	1.16	15.88	4.67	2.93	0.38	1.1	2.88	0.20	b.d.l	12.18

In the end, the research confirms the influence of the silt mineralogy on the deflocculation/coagulation process and brings new questions regarding its robustness, as the nature of the suspension can act negatively on the entire process. Research is particularly needed on this mechanism to better apprehend it through the diversity of soil and its uses in earthen construction.

CRedit authorship contribution statement

Nino Zosso: Investigation. **Coralie Brumaud:** Writing – review & editing, Supervision, Methodology, Conceptualization. **Ellina Bernard:** Writing – review & editing, Methodology, Investigation. **Guillaume Habert:** Writing – review & editing, Supervision, Methodology, Conceptualization. **Daria Ardant:** Writing – review & editing, Writing – original draft, Methodology, Investigation, Conceptualization.

Declaration of Competing Interest

The authors declare that they have no known competing financial interests or personal relationships that could have appeared to influence the work reported in this paper.

Data Availability

No data was used for the research described in the article.

Acknowledgements

Ellina Bernard acknowledges the financial support by the Swiss National Science Foundation (SNSF project no. PZ00P2_201697). The NMR hardware was partially granted by the Swiss National Science Foundation (SNSF, grant no. 206021_150638/1).

References

- J.C. Morel, A. Mesbah, M. Oggero, P. Walker, Building houses with local materials: means to drastically reduce the environmental impact of construction, *Build. Environ.* 36 (2001) 1119–1126, [https://doi.org/10.1016/S0360-1323\(00\)00054-8](https://doi.org/10.1016/S0360-1323(00)00054-8).
- A. Fabbri, J.-C. Morel, J.-E. Aubert, Q.-B. Bui, D. Gallipoli, B.V.V. Reddy, eds., Testing and Characterisation of Earth-based Building Materials and Elements, 35 (2022). <https://doi.org/10.1007/978-3-030-83297-1>.
- R. Charef, J.C. Morel, K. Rakhshan, Barriers to implementing the circular economy in the construction industry: a critical review, 2021, Vol. 13, Page 12989, *Sustainability* 13 (2021) 12989, <https://doi.org/10.3390/SU132312989>.
- L. Verron, E. Hamard, B. Cazacliu, A. Razakamanantsoa, M. Duc, T. Vincelas, A. Hellouin de Menibus, B. Lemerrier, R.J. Ansaa-Asare, T. Lecomte, Estimating and mapping the availability of earth resource for light earth building using a soil geodatabase in Brittany (France), *Resour. Conserv. Recycl.* 184 (2022) 106409, <https://doi.org/10.1016/J.RESCONREC.2022.106409>.
- M. Moëvus, L. Fontaine, R. Anger, P. Doat, P. Doat Projet, Projet: Béton d'Argile Environnemental (B.A.E.), 2013. (<https://hal.archives-ouvertes.fr/hal-01179451>) (accessed January 25, 2021).
- H. Van Damme, H. Houben, Earth concrete. Stabilization revisited, *Cem. Concr. Res.* 114 (2018) 90–102, <https://doi.org/10.1016/j.cemconres.2017.02.035>.
- C. Brumaud, Y. Du, D. Ardant, G. Habert, Earth, the new liquid stone: development and perspectives, *Mater. Today Commun.* (2024) 108959, <https://doi.org/10.1016/J.MTCOMM.2024.108959>.
- L. Fontaine, R. Anger, Grains de bâtisseurs. Bâtir en terre, du grain de sable à l'architecture, Belin, 2010.
- C.M. Ouellet-Plamondon, G. Habert, Self-compacted clay based concrete (SCCC): Proof-of-concept, *J. Clean. Prod.* 117 (2016) 160–168, <https://doi.org/10.1016/j.jclepro.2015.12.048>.
- M. Moëvus, Y. Jorand, C. Olagnon, S. Maximilien, R. Anger, L. Fontaine, L. Arnaud, Earthen construction: an increase of the mechanical strength by optimizing the dispersion of the binder phase, *Mater. Struct. Constr.* 49 (2016) 1555–1568, <https://doi.org/10.1617/s11527-015-0595-5>.
- Y. Du, C. Brumaud, F. Winnefeld, Y.H. Lai, G. Habert, Mechanisms for efficient clay dispersing effect with tannins and sodium hydroxide, *Colloids Surf. A Physicochem. Eng. Asp.* 630 (2021) 127589, <https://doi.org/10.1016/J.COLSURFA.2021.127589>.
- G. Landrou, C. Brumaud, F. Winnefeld, R.J. Flatt, G. Habert, Lime as an anti-plasticizer for self-compacting clay concrete, *Mater. ials* 9 (2016), <https://doi.org/10.3390/ma9050330>.
- G. Landrou, C. Brumaud, M.L. Plötze, F. Winnefeld, G. Habert, A fresh look at dense clay paste: deflocculation and thixotropy mechanisms, *Colloids Surf. A Physicochem. Eng. Asp.* 539 (2018) 252–260, <https://doi.org/10.1016/j.colsurfa.2017.12.029>.
- D. Ardant, C. Brumaud, G. Habert, Influence of additives on poured earth strength development, *Mater. Struct. Constr.* 53 (2020) 1–17, <https://doi.org/10.1617/s11527-020-01564-y>.
- A. Pinel, Y. Jorand, C. Olagnon, A. Charlot, E. Fleury, Towards poured earth construction mimicking cement solidification: demonstration of feasibility via a biosourced polymer, *Mater. Struct. Constr.* 50 (2017) 1–17, <https://doi.org/10.1617/s11527-017-1092-9>.
- A. Pinel, E. Prud'homme, A. Charlot, E. Fleury, Y. Jorand, Earthen Construction: Demonstration of Feasibility at 1/2 Scale of Poured Clay Concrete Construction, (2021). <https://doi.org/10.1016/j.conbuildmat.2021.125275>.
- J.R. Clausell, C.H. Signes, G.B. Solà, B.S. Lanzas, Improvement in the rheological and mechanical properties of clay mortar after adding Ceratonia siliqua L. extracts, *Constr. Build. Mater.* 237 (2020), <https://doi.org/10.1016/j.conbuildmat.2019.117747>.
- G. Landrou, C. Brumaud, G. Habert, Influence of magnesium on deflocculated kaolinite suspension: mechanism and kinetic control, *Colloids Surf. A Physicochem. Eng. Asp.* 544 (2018) 196–204, <https://doi.org/10.1016/j.colsurfa.2017.12.040>.
- F. Andreola, E. Castellini, T. Manfredini, M. Romagnoli, The role of sodium hexametaphosphate in the dissolution process of kaolinite and kaolin, *J. Eur. Ceram. Soc.* 24 (2004) 2113–2124, [https://doi.org/10.1016/S0955-2219\(03\)00366-2](https://doi.org/10.1016/S0955-2219(03)00366-2).
- L. Liang, T. Zhang, Y. Peng, G. Xie, Inhibiting heterocoagulation between microcrystalline graphite and quartz by pH modification and sodium hexametaphosphate, *Colloids Surf. A Physicochem. Eng. Asp.* 553 (2018) 149–154, <https://doi.org/10.1016/J.COLSURFA.2018.05.045>.
- M. Kohandelnia, M. Hosseini, A. Yahia, R. Belarbi, A new approach for proportioning self-consolidating earth paste (SCEP) using the Taguchi method, *Constr. Build. Mater.* 347 (2022) 128579, <https://doi.org/10.1016/J.CONBUILDMAT.2022.128579>.
- M. Kohandelnia, M. Hosseini, A. Yahia, R. Belarbi, Multiscale investigation of self-consolidating earthen materials using a novel concrete-equivalent mortar approach, *Constr. Build. Mater.* 370 (2023) 130700, <https://doi.org/10.1016/J.CONBUILDMAT.2023.130700>.
- ISO - ISO 11277:2020 - Soil quality — Determination of Particle Size Distribution in Mineral Soil Material — Method by Sieving and Sedimentation, (n.d.). (<https://www.iso.org/standard/69496.html>) (accessed September 22, 2021).
- D. Bish, M. Plötze, X-Ray Powder Diffraction, *Emphas. Qual. Anal. Ind. Mineral.* (2010). (<https://pubs.geoscienceworld.org/books/edited-volume/940/chapter/106814543>) (accessed November 20, 2023).
- N. Doebelin, R. Kleeberg, Profex: A Graphical User Interface for the Rietveld Refinement Program BGMN, *Urn:Issn:1600-5767*. 48 (2015) 1573–1580. <https://doi.org/10.1107/S1600576715014685>.
- N. Roussel, Understanding the Rheology of Concrete, Woodhead, 2011, <https://doi.org/10.1533/9780857095282>.
- Q.D. Nguyen, D.V. Boger, Measuring the flow properties of yield stress fluids, *Annu. Rev. Fluid Mech.* 24 (1992) 47–88, <https://doi.org/10.1146/annurev.fl.24.010192.000403>.
- C. Brumaud, R. Baumann, M. Schmitz, M. Radler, N. Roussel, Cellulose ethers and yield stress of cement pastes, *Cem. Concr. Res.* 55 (2014) 14–21, <https://doi.org/10.1016/j.cemconres.2013.06.013>.
- A.W. Saak, H.M. Jennings, S.P. Shah, The influence of wall slip on yield stress and viscoelastic measurements of cement paste, *Cem. Concr. Res.* 31 (2001) 205–212, [https://doi.org/10.1016/S0008-8846\(00\)00440-3](https://doi.org/10.1016/S0008-8846(00)00440-3).
- A. Zingg, F. Winnefeld, L. Holzer, J. Pakusch, S. Becker, R. Figi, L. Gauckler, Interaction of polycarboxylate-based superplasticizers with cements containing different C3A amounts, *Cem. Concr. Compos.* 31 (2009) 153–162, <https://doi.org/10.1016/J.CEMCONCOMP.2009.01.005>.
- G. Lagaly, I. Dékány, Colloid Clay Science, 2013. <https://doi.org/10.1016/B978-0-08-098258-8.00010-9>.
- R.J. Hunter, S.K. Nicol, The dependence of plastic flow behavior of clay suspensions on surface properties, *J. Colloid Interface Sci.* 28 (1968).
- A. Yamaguchi, M. Kobayashi, Y. Adachi, Yield Stress of Mixed Suspension of Silica Particles and Lysozymes: The Effect of Zeta Potential and Adsorbed Amount, (2019). <https://doi.org/10.1016/j.colsurfa.2019.123575>.
- E.L. Sjöberg, A fundamental equation for calcite dissolution kinetics, *Geochim. Cosmochim. Acta* 40 (1976) 441–447, [https://doi.org/10.1016/0016-7037\(76\)90009-0](https://doi.org/10.1016/0016-7037(76)90009-0).
- G. Kura, S. Ohashi, Complex formation of cyclic phosphate anions with bivalent cations, *J. Inorg. Nucl. Chem.* 36 (1974) 1605–1609.
- W.A. Deer, R.A. Howie, J. Zussman, An introduction to the rock-forming minerals, *Introd. Rock. Form. Miner.* (2013), <https://doi.org/10.1180/DHZ>.
- F. Andreola, E. Castellini, J.M.F. Ferreira, S. Olhero, M. Romagnoli, Effect of sodium hexametaphosphate and ageing on the rheological behaviour of kaolin dispersions, *Appl. Clay Sci.* 31 (2006) 56–64, <https://doi.org/10.1016/J.CLAY.2005.08.004>.
- M. Braun, P. Hartmann, C. Jana, 19F and 31P NMR spectroscopy of calcium apatites, *J. Mater. Sci. Mater. Med.* 6 (1995) 150–154, <https://doi.org/10.1007/BF00120291>.
- S. Greenfield, Analytical Chemistry of the Condensed Phosphates, 1st ed., Pergamon Press, Oxford, 1975 <https://doi.org/10.1016/c2013-0-10082-7>.

- [40] E. Bernard, M. Yio, D. Rentsch, H. Chen, R.J. Myers, Insights on the effects of carbonates and phosphates on the hydration of magnesia (alumino-)silicate cements, *Appl. Geochem.* 167 (2024) 106001, <https://doi.org/10.1016/J.APGEOCHEM.2024.106001>.
- [41] C. Liu, M. Zhang, G. Pan, L. Lundehøj, U.G. Nielsen, Y. Shi, H.C.B. Hansen, Phosphate capture by ultrathin MgAl layered double hydroxide nanoparticles, *Appl. Clay Sci.* 177 (2019) 82–90, <https://doi.org/10.1016/J.CLAY.2019.04.019>.
- [42] C. Jäger, T. Welzel, W. Meyer-Zaika, M. Epple, A solid-state NMR investigation of the structure of nanocrystalline hydroxyapatite, *Magn. Reson. Chem.* 44 (2006) 573–580, <https://doi.org/10.1002/MRC.1774>.
- [43] F.J. Huertas, L. Chou, R. Wollast, Mechanism of kaolinite dissolution at room temperature and pressure Part II: kinetic study, *Geochim. Cosmochim. Acta* 63 (1999) 3261–3275, [https://doi.org/10.1016/S0016-7037\(99\)00249-5](https://doi.org/10.1016/S0016-7037(99)00249-5).
- [44] F.J. Huertas, L. Chou, R. Wollast, Mechanism of Kaolinite dissolution at room temperature and pressure: Part 1. surface speciation, *Geochim. Cosmochim. Acta* 62 (1998) 417–431, [https://doi.org/10.1016/S0016-7037\(97\)00366-9](https://doi.org/10.1016/S0016-7037(97)00366-9).